Physics Letters B 729 (2014) 27–32

Contents lists available at ScienceDirect

Physics Letters B

www.elsevier.com/locate/physletb

Spin-dipole nuclear matrix elements for double beta decays and astro-neutrinos

H. Ejiri [a,b,*], N. Soukouti [c], J. Suhonen [c]

[a] Research Center for Nuclear Physics, Osaka University, Ibaraki, Osaka, 567-0047, Japan
[b] Nuclear Science, Czech Technical University, Prague, Czech Republic
[c] Department of Physics, P.O. Box 35 (YFL), FI-40014 University of Jyväskylä, Finland

ARTICLE INFO

Article history:
Received 25 October 2013
Received in revised form 13 December 2013
Accepted 18 December 2013
Available online 27 December 2013
Editor: W. Haxton

Keywords:
Spin-dipole matrix element
Unique forbidden beta decay
Double beta decay
Renormalization of the axial-vector weak coupling constant

ABSTRACT

Spin-dipole (SD) nuclear matrix elements (NMEs) $M^{\pm}$(SD2) for unique first forbidden $\beta^{\pm}$ $2^- \rightarrow 0^+$ ground-state-to-ground-state transitions are studied by using effective microscopic two-nucleon interactions in realistic single-particle model spaces. The observed values of the NMEs $M^{\pm}_{\rm exp}$(SD2) are compared with the values of the single-quasiparticle NMEs $M^{\pm}_{\rm qp}$(SD2) without nucleon spin–isospin $(\sigma\tau)$ correlation and the QRPA NMEs $M^{\pm}_{\rm QRPA}$(SD2) with the $\sigma\tau$ correlation. The observed SD matrix elements are found to be reduced by the factor $k \approx 0.2$ with respect to $M^{\pm}_{\rm qp}$(SD2) and by the factor $k_{\rm NM} \approx 0.5$ with respect to $M^{\pm}_{\rm QRPA}$(SD2). We then infer that the SD NME is reduced considerably partly by the nucleon $\sigma\tau$ correlations and partly by other non-nucleonic and nucleonic correlations which are not explicitly included in the QRPA. Impact of the found reduction factors on the magnitudes of the NMEs involved in neutrino-less double beta decays and astro-neutrino interactions are discussed.

Fundamental properties of neutrinos and their interactions can be studied by investigating neutrino-less double beta ($0\nu\beta\beta$) decays and astro-neutrino–nuclear processes. Here the associated nuclear matrix elements (NMEs) are crucial to extract quantitative neutrino properties that are of interest to particle and astrophysics, as discussed in reviews [1–6] and refs. therein.

The present Letter aims to analyze the spin-dipole (SD) $\beta^{\pm}$ NMEs for $2^- \rightarrow 0^+$ ground-state-to-ground-state transitions and to compare them with current model calculations. These NMEs are associated with the $J^{\pi} = 2^-$ component of the $0\nu\beta\beta$ matrix element and the cross sections of the medium-energy neutrino–nuclear interactions. We show that the SD matrix elements are considerably reduced due to nucleonic spin(σ)–isospin(τ) and other correlations as well as possible non-nucleonic nuclear medium effects.

The $0\nu\beta\beta$ decays of several isotopes are under extensive experimental and theoretical study to access the Majorana properties of neutrinos and their absolute mass scales [2–5]. Then a reliable value of the $0\nu\beta\beta$ NME, $M^{0\nu}$, is required to design an optimum $0\nu\beta\beta$ detector and to deduce the neutrino mass from the measured $0\nu\beta\beta$ decay rate in case it is observed. In fact, exact theoretical evaluations for $M^{0\nu}$ are hard [2,6,7], and thus comprehensive model calculations using appropriate nuclear interactions and the renormalized weak coupling constant $g_{\rm A}$ are necessary to get accurate values for $M^{0\nu}$ [7,8].

In case of the light-neutrino mediated $0\nu\beta\beta$ decay a virtual Majorana neutrino is exchanged between two nucleons of the mother nucleus. Then the momentum of the virtual neutrino is around $q \approx 100$–50 MeV/c and the angular momenta involved in the process are mainly $l\hbar = 1\hbar - 3\hbar$ and the spin and parity of the intermediate states are $J^{\pm} = 1^{\pm} - 4^{\pm}$. Among them one of the largest components is $J^{\pi} = 2^-$ associated with the p-wave neutrino axial-vector (AV) interaction [7]. The NMEs relevant to this virtual-neutrino interaction are the β^- and β^+ matrix elements of M^+_i(SD2) and M^-_i(SD2) with i standing for the ith intermediate state. Thus the single β NME M(SD2) is of great interest due to its intimate relation with $M^{0\nu}$, as discussed in review articles [2,4,9] and also in a workshop proceedings [10].

Astro-neutrino charged-current (CC) interaction rates are given by inverse $\beta^{\pm}$ decay rates. Then the $\beta^{\pm}$ NME is needed to derive the neutrino flux from the interaction rate and vice versa. The supernova neutrino energy extends up to a few tens of MeV, and then the NME $M^{\pm}$(SD2) associated with the p-wave neutrino AV interaction gets relatively important [11–13].

* Corresponding author at: Research Center for Nuclear Physics, Osaka University, Ibaraki, Osaka 567-0047, Japan.
E-mail addresses: ejiri@rcnp.osaka-u.ac.jp (H. Ejiri), nael.n.soukouti@student.jyu.fi (N. Soukouti), jouni.suhonen@phys.jyu.fi (J. Suhonen).

http://dx.doi.org/10.1016/j.physletb.2013.12.051

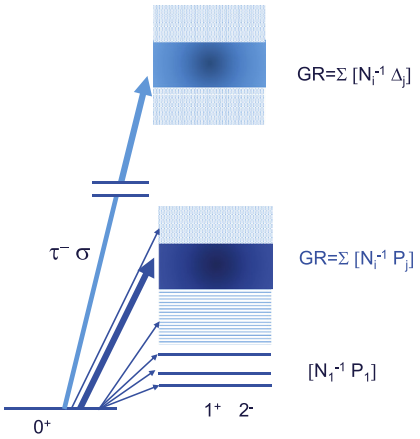

Fig. 1. Schematic diagram of isospin–spin strengths for low-lying nuclear states and spin–isospin giant resonances (GR). Nucleon particle–hole GRs with $J^\pi = 1^+, 2^-$ are located around 12–25 MeV region, while isobar nucleon-hole GRs are at around 300 MeV (see text).

The 2^- single β transition strength is given as

$$B^{\pm}(\mathrm{SD2}) = \frac{1}{2J_i+1}\left|M^{\pm}(\mathrm{SD2})\right|^2, \tag{1}$$

where J_i is the initial state spin and $M^{\pm}(\mathrm{SD2})$ is the reduced SD matrix element. It is expressed as

$$M^{\pm}(\mathrm{SD2}) = \left\langle f \left\| \tau^{\pm}[\sigma \times rY_1]_2 \right\| i \right\rangle, \tag{2}$$

where $\tau^{\pm}$ are the isospin operators for $\beta^{\pm}$ and σ is the Pauli spin operator.

The SD 2^- matrix elements have been studied by investigating forbidden β and M2 γ decays as discussed in Refs. [14–18]. The SD matrix elements are shown to be reduced by the repulsive $\tau\sigma$ interaction which pushes the 2^- strength up to the possible SD 2^- giant resonance (SDGR). The SDGRs are expressed as coherent sums of nucleon-particle–nucleon-hole SD states [18]. The observed SD NME is suggested to be reduced further since the strength is pushed up to the possible isobar GR, which is expressed as a coherent sum of nucleon-hole–Δ-particle SD states at the 300 MeV region [19]. SD strengths spread over other states as well. The reduction is a common feature of $\tau\sigma$ weak and electro-magnetic transitions [18]. The SD strength distributions are schematically shown in Fig. 1.

The Gamow–Teller (GT) 1^+ NME involved in the s-wave $\tau\sigma$ interaction is the major player in the low-energy s-wave neutrino processes such as the two-neutrino double beta ($2\nu\beta\beta$) decays and low-energy astro-neutrino–nuclear interactions. The single β GT strengths have been studied by measuring allowed β decays and charge exchange reactions (CERs), such as (p, n), (n, p), (d, ^{2}He), (^{3}He, t) (t, ^{3}He) and others. They were studied at IUCF, KVI, LAMPF, NSCL, RCNP, RIKEN, TRIUMP, UC-Davis, Uppsala Univ., and many other labs. as given in the references of reviews [1,2,4].

Recently, precision studies of individual low-lying GT and SD states were made by using the high energy-resolution ($\Delta E/E \approx 5\times10^{-5}$) spectrometer at RCNP. The (^{3}He, t) CERs were studied on $\beta\beta$ nuclei [20–26]. The observed spectra show clearly distinct GT 1^+ and SD 2^- peaks in the low-excitation region and broad GT 1^+ GR and SD 2^- GR in the high-excitation region around 15–25 MeV, as shown in Fig. 1. So far, the GT strengths for individual states were extracted from their data. The $2\nu\beta\beta$ NMEs ($M^{2\nu}$) are reproduced by using experimental single β GT NMEs of $M^{\pm}(\mathrm{GT1}^+)$ [2,27,28]. The renormalization of g_A in $2\nu\beta\beta$ has been discussed theoretically in [29,30]. Also these analyses show renormalization (quenching) factors of around 0.4–0.6.

Table 1
SD 2^- NMEs for β^- and β^+(EC) decays in the mass region of $A = 72$–86, where the major single-quasiparticle transition is $1g_{9/2} - 1f_{5/2}$. M_{exp}, M_{qp} and M_{QRPA} are the experimental, single-quasiparticle, and QRPA NMEs in units of nu (natural unit) $\times10^{-3}$.

Transition	Mode	M_{exp}	M_{qp}	M_{QRPA}
^{72}As → ^{72}Ge	β^+	1.43	14.7	2.94
^{74}As → ^{74}Se	β^-	2.42	9.77	7.21
^{74}As → ^{74}Ge	β^+	1.68	14.6	4.87
^{76}As → ^{76}Se	β^-	1.60	8.80	6.07
^{78}As → ^{78}Se	β^-	1.80	7.74	3.91
^{84}Br → ^{84}Kr	β^-	2.18	7.35	4.93
^{84}Rb → ^{84}Kr	β^+	2.08	15.2	3.96
^{84}Rb → ^{84}Sr	β^-	2.18	8.48	5.53
^{86}Rb → ^{86}Sr	β^-	2.26	7.79	5.60
^{86}Rb → ^{86}Kr	β^+	1.53	15.6	4.34

Table 2
The same as Table 1 for $A = 88$–94, where the major single-quasiparticle transition is $2d_{5/2} - 2p_{1/2}$.

Transition	Mode	M_{exp}	M_{qp}	M_{QRPA}
^{88}Rb → ^{88}Sr	β^-	2.85	7.98	4.06
^{92}Y → ^{92}Zr	β^-	2.85	6.97	4.55
^{94}Y → ^{94}Zr	β^-	2.51	6.68	3.57

Table 3
The same as Table 1 for $A = 122$–132, where the major single-quasiparticle transition is $1h_{11/2} - 1g_{7/2}$.

Transition	Mode	M_{exp}	M_{qp}	M_{QRPA}
^{122}Sb → ^{122}Sn	β^+	3.75	19.9	9.40
^{122}Sb → ^{122}Te	β^-	1.77	11.2	2.65
^{124}I → ^{124}Te	β^+	2.74	19.8	8.38
^{126}I → ^{126}Te	β^+	3.22	20.0	9.62
^{126}I → ^{126}Xe	β^-	1.58	9.30	2.68
^{132}La → ^{132}Ba	β^+	2.12	19.9	8.88

Extraction of the SD single $\beta^{\pm}$ strength from the CER data is not straightforward. Thus we analyze the SD strength from the observed f_1t value for the unique first-forbidden $\beta^{\pm}$ decay. It is given by

$$B^{\pm}(\mathrm{SD2}) = \frac{9D}{4\pi f_1 t}\left(\frac{g_{\mathrm{V}}}{g_{\mathrm{A}}}\right)^2, \tag{3}$$

where D contains the weak coupling strength and $g_{\mathrm{V}}/g_{\mathrm{A}} = 1/1.267$ [31] is the ratio of the vector and axial-vector coupling constants. The experimental SD matrix element $M_{\mathrm{exp}}(\mathrm{SD2})$ is derived from the observed SD strength by using Eq. (1). Actually, τ^+ β decays in medium-heavy-mass nuclei are EC (electron capture) processes, and thus the β^+ strengths are derived from the EC rates.

Isotopes used for on-going and/or future $\beta\beta$ experiments are ^{76}Ge, ^{82}Se, ^{100}Mo, ^{116}Cd, ^{130}Te and ^{136}Xe. They are in the mass regions of $A = 70$–86, $A = 88$–120 and $A = 130$–140, respectively. The major SD transitions in these mass regions are $1g_{9/2}$–$1f_{5/2}$, $2d_{5/2}$–$2p_{1/2}$ and $1h_{11/2}$–$1g_{7/2}$, respectively. Their single-particle SD NMEs are quite large because of the large radial and angular overlap integrals. The single $\beta^{\pm}$ $2^- \to 0^+$ SD NMEs for nuclei in the three mass regions are derived from the f_1t values [32] as given in the third column of Tables 1, 2 and 3 in natural units (nu) of nu $= \hbar/m_ec = 383$ fm. The observed values for $M_{\mathrm{exp}}(\mathrm{SD2})$ are around $(2.4\pm1.2)\times10^{-3}$ nu, as shown in Fig. 2. The NMEs region corresponds to a band of $\log f_1t \approx 9.4\pm0.3$, which is much smaller than typical spreads of around ±1.5 for other β decay $\log ft$ values in medium and heavy nuclei [32].

In the simplest picture the β decays discussed here proceed between single-quasiparticle states. Then the NMEs are written by

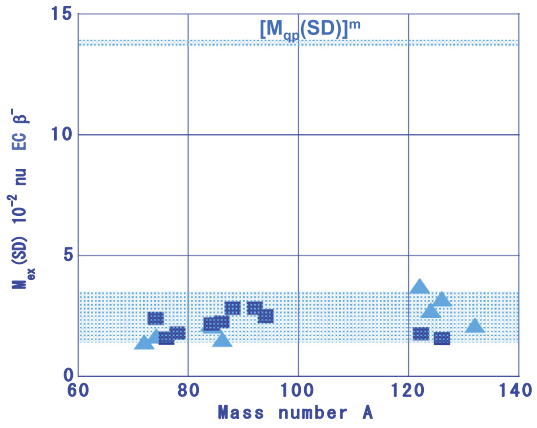

Fig. 2. SD 2^- NMEs for the ground-state-to-ground-state $2^- \to 0^+$ decays. The observed matrix elements $M_{\rm exp}$(SD2) for β^- (squares) and β^+ (triangles) decays are plotted against the mass number A. $[M_{\rm qp}({\rm SD2})]^{\rm m}$ is the mean value of the single-quasiparticle NMEs.

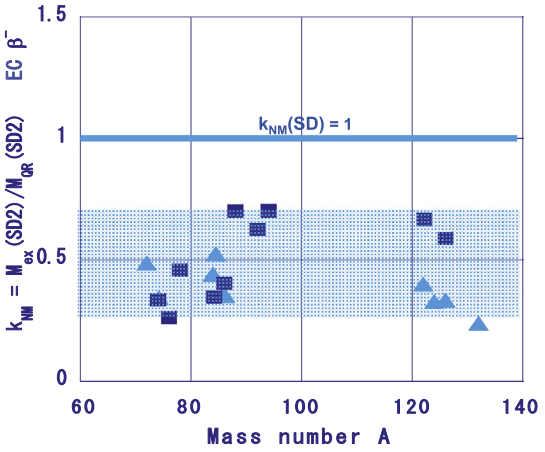

Fig. 3. Ratios $k_{\rm NM}$ of the observed NME $M_{\rm exp}$(SD2) and the QRPA NME $M_{\rm QRPA}$(SD2) for the ground-state-to-ground-state $2^- \to 0^+$ transitions are plotted against the mass number A. Squares and triangles are the ratios for the β^- and β^+ transitions, respectively.

using the single-particle matrix element $M_{\rm sp}$(SD2) and the pairing factor P as

$$M_{\rm qp}({\rm SD2}) = M_{\rm sp}({\rm SD2})P. \tag{4}$$

The pairing factor P is given as $P = U_n V_p$ and $P = U_p V_n$ for β^- and β^+ decays respectively, where U_p (U_n) and V_p (V_n) are the vacancy and occupation amplitudes for the proton (neutron) in the final nucleus. The single-quasiparticle NMEs are evaluated by using the harmonic-oscillator single-particle wave functions and the BCS-based U and V factors. The evaluated NMEs are given in the fourth column of Tables 1, 2 and 3. Here the BCS values for U and V are obtained by using the single-particle energies in [33] and the pairing interaction from a realistic G-matrix, which reproduces well global pairing features of low lying states and the pairing gaps derived from experimental separation energies for protons and neutrons.

The single-quasiparticle NMEs are rather scattered around the mean value of $M_{\rm qp}({\rm SD2})^{\rm m} \approx 13.5$. The observed NMEs are far below the single-quasiparticle NMEs as seen in Fig. 2. The relation between these two NMEs can be expressed in terms of a reduction factor k as

$$M_{\rm exp}({\rm SD2}) = kM_{\rm qp}({\rm SD2}). \tag{5}$$

The k coefficients are scattered around $k \approx 0.2$ and they may be considered to stand for the reduction due to the $\tau\sigma$ correlation and nuclear medium effects and others, if any, which are not explicitly included in the QP model.

The realistic SD 2^- NMEs were calculated in terms of the quasiparticle RPA (QRPA) model with the $\tau\sigma$ correlation (the proton–neutron QRPA, i.e. pnQRPA). The corresponding NMEs are shown in the fifth column of Tables 1, 2 and 3. The adopted single-particle spaces are large enough to stabilize the value of the SD 2^- NME for the ground-state-to-ground-state transition. The adopted proton–neutron interaction is based on the realistic G-matrix, where the pairing and multipole channels are scaled by few constants as explained in [34–36]. For the multipole channels the particle–hole interaction is scaled by a strength constant g_{ph} such that the centroid of the observed GTGR is reproduced. It should be noted that the low-lying SD 2^- strength is quite insensitive to the particle–particle interaction constant g_{pp} in contrast to the low-lying GT 1^+ strength [37].

The observed SD NMEs are found to be significantly reduced with respect to the QRPA values by the reduction factor $k_{\rm NM}$ with values around 0.5 for both the β^- and β^+(EC) transitions, as shown in Fig. 3. The reduction can be written as

$$M_{\rm exp}({\rm SD2}) = k_{\rm NM} M_{\rm QRPA}({\rm SD2}), \tag{6}$$

where the reduction factor of $k_{\rm NM} \approx 0.5$ suggests that the SD axial weak coupling is reduced in nuclei due to some nuclear medium effects which are not explicitly included in the QRPA.

The reduction factor for the SD matrix element may be expressed as

$$k \approx k_{\tau\sigma} \times k_{\rm NM}, \tag{7}$$

where $k \approx 0.2$, $k_{\tau\sigma} \approx 0.4$ and $k_{\rm NM} \approx 0.5$. These values depend little on the nuclear parameters used for the present quasiparticle and QRPA models.

Actually, the values of the SD matrix elements depend on the nucleon configurations at the nuclear Fermi surface, i.e. on the occupation and vacancy amplitudes of V and U. The reduction due to the nucleon $\sigma\tau$ correlations and other non-nucleonic renormalization effects such as the isobar correlations are nuclear core/medium effects. In order to elucidate such nuclear core/medium effects, we consider the geometric mean of the β^+ and β^- NMEs for the available cases where both of them have been measured. The mean value is expressed as

$$M^{\rm m}({\rm SD2}) = \left[M^+({\rm SD2})M^-({\rm SD2})\right]^{1/2}, \tag{8}$$

where $M^{\pm}$(SD2) is the reduced matrix element for the $\beta^{\pm}$ transition $A(Z,N) \leftrightarrow A(Z \mp 1, N \pm 1)$. In fact there are two types of such decays, one common odd–odd nucleus decays to two neighboring even–even nuclei, and two neighboring odd–odd nuclei decay to one common even–even nucleus. In terms of the quasiparticle expression, the mean matrix element is expressed as

$$M^{\rm m}_{\rm qp}({\rm SD2}) = M_{\rm sp}({\rm SD2})\left(V_p U_n V'_n U'_p\right)^{1/2}, \tag{9}$$

where V_p, U_n and V'_n, U'_p are the pairing factors for the β^+ and β^- final nuclei. Noting that $U'_i \approx \sqrt{1 - V_i^2}$ and $V'_i \approx \sqrt{1 - U_i^2}$, with i being p or n, the geometric mean of the pairing factor is given as $(V_p U_n V'_n U'_p)^{1/2} \approx 0.43 \pm 0.05$ in a wide range of U and V. In other words, the nuclear surface effects due to the valence nucleon configurations are averaged in the mean NME. Thus the geometric mean is very insensitive to the nucleon configuration at the Fermi surface, but rather reflects the nuclear core/medium effects. The mean values are obtained for 6 $\beta^{\pm}$ decays as shown in Table 4.

Table 4
Mean SD 2^- NMEs derived from the $\beta^\pm$ matrix elements given in Tables 1, 2 and 3. $M^{\rm m}_{\rm exp}$, $M^{\rm m}_{\rm qp}$ and $M^{\rm m}_{\rm QRPA}$ are the geometric mean values of the experimental, single quasiparticle, and QRPA matrix elements in nu (natural unit) $\times 10^{-3}$. The effective reduction factors are $k^{\rm m} = M^{\rm m}_{\rm exp}/M^{\rm m}_{\rm qp}$ and $k^{\rm m}_{\rm NM} = M^{\rm m}_{\rm exp}/M^{\rm m}_{\rm QRPA}$.

Common nucleus	$M^{\rm m}_{\rm exp}$	$M^{\rm m}_{\rm qp}$	$M^{\rm m}_{\rm QRPA}$	$k^{\rm m}$	$k^{\rm m}_{\rm NM}$
^{74}As	2.02	11.9	5.93	0.169	0.341
^{84}Kr	2.13	10.6	4.42	0.201	0.481
^{84}Rb	2.13	11.4	4.68	0.188	0.429
^{86}Rb	1.86	11.0	4.93	0.169	0.377
^{122}Sb	2.58	14.9	4.99	0.173	0.517
^{126}I	2.26	13.6	5.08	0.166	0.445

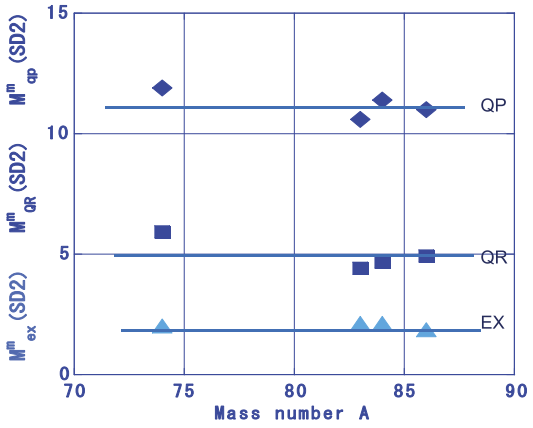

Fig. 4. Mean SD 2^- NMEs for the ground state $2^- \to 0^+$ $\beta^\pm$ transitions in nuclei with $A = 74$–86. $M^{\rm m}_{\rm exp}$, $M^{\rm m}_{\rm qp}$ and $M^{\rm m}_{\rm QRPA}$ are mean values of the observed NMEs (EX triangles), the quasiparticle NMEs (QP diamonds) and the QRPA NMEs (QR squares). The values for ^{84}Kr are plotted at $A = 83$ to avoid overlaps with those of ^{84}Rb.

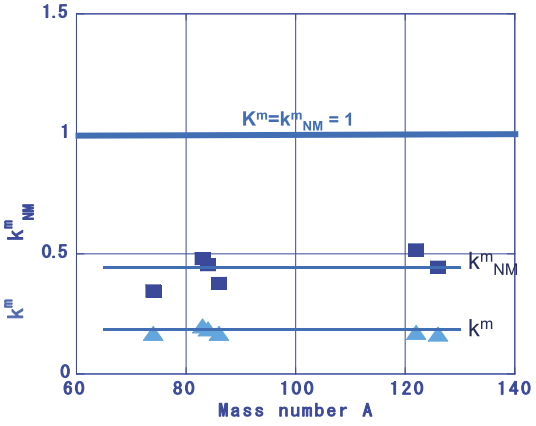

Fig. 5. Effective reduction factors $k^{\rm m}$ (triangles) and $k^{\rm m}_{\rm NM}$ (diamonds) for the mean SD 2^- NMEs. They are defined as $k^{\rm m} = M^{\rm m}_{\rm exp}/M^{\rm m}_{\rm qp}$ and $k^{\rm m}_{\rm NM} = M^{\rm m}_{\rm exp}/M^{\rm m}_{\rm QRPA}$. The values for ^{84}Kr are plotted at $A = 83$ to avoid overlaps with those of ^{84}Rb.

The mean NMEs are plotted against the mass number in Figs. 4 and 5. It is remarkable to see that the mean NMEs are not scattered unlike the individual NMEs given in Tables 1, 2 and 3, and in Figs. 2 and 3, but they are nearly the same for all nuclei. The mean NMEs are approximately given by

$$M^{\rm m}_{\rm exp}({\rm SD2}) \approx 2.2 \times 10^{-3}\ {\rm nu}, \tag{10}$$

$$M^{\rm m}_{\rm qp}({\rm SD2}) \approx 12 \times 10^{-3}\ {\rm nu}, \tag{11}$$

$$M^{\rm m}_{\rm QRPA}({\rm SD2}) \approx 5.0 \times 10^{-3}\ {\rm nu}. \tag{12}$$

They are expressed by using the effective reduction factors of $k^{\rm m}$ and $k^{\rm m}_{\rm NM}$ as

$$M^{\rm m}_{\rm exp} \approx k^{\rm m} M_{\rm qp}, \quad k^{\rm m} \approx 0.18, \tag{13}$$

$$M^{\rm m}_{\rm exp} \approx k^{\rm m}_{\rm NM} M_{\rm QRPA}, \quad k^{\rm m}_{\rm NM} \approx 0.45, \tag{14}$$

$$k^{\rm m} = k^{\rm m}_{\tau\sigma} \times k^{\rm m}_{\rm NM}, \quad k^{\rm m}_{\tau\sigma} \approx 0.4. \tag{15}$$

We note that these effective reduction factors are rather independent of nuclear parameters used in the quasiparticle and QRPA models.

In short, the present analyses show that the SD 2^- weak NMEs, which play important roles for the $0\nu\beta\beta$ NMEs and the astro-neutrino inverse-β NMEs, are much reduced by reduction factors of $k \approx 0.2$ and $k_{\rm NM} \approx 0.5$ with respect to the single-quasiparticle values and the standard QRPA calculations, respectively, in medium heavy nuclei. The reductions are considered to be due to the $\tau\sigma$ correlation effect of $k_{\tau\sigma} \approx 0.4$ and the other nuclear medium and correlation effect of $k_{\rm NM} \approx 0.5$. The latter is associated with the non-nucleonic (isobar) and other correlations, which are not included in the standard QRPA. Then this may be incorporated by using an effective $g_{\rm A}^{\rm eff} \approx 0.5 g_{\rm A}$ in the standard QRPA.

Let us discuss the present results and their impacts on the $0\nu\beta\beta$ NMEs and astro-ν interactions.

The 2^- ground states discussed here are all simple quasiparticle states with the unique configuration of $(l + 1/2, l' - 1/2)$ with $l' = l - 1$. The β transitions are single-quasiparticle ones of $(l + 1/2) \leftrightarrow (l' - 1/2)$ with a large single-particle NME. The quasiparticle NME depends on the quasiparticle U and V factors, but the effects are minimized in the geometrical mean of the $M^{\pm}({\rm SD2}^-)$. There are no other strong SD states nearby, and thus couplings with other states are not appreciable. They are included in the QRPA calculations.

The present QRPA calculations are based on Woods–Saxon single-particle energies with the global Bohr–Mottelson parametrization [33]. These parameters are fitted to reproduce the properties of nuclei close to the stability line of the nuclear chart and thus suitable for the present calculations. The Woods–Saxon energies vary smoothly and so do the computed NMEs in general. Deviations from the smooth trend occur in some cases where the computed NME is very small (the $A = 72, 122(\beta^-), 126$ cases) but then also the observed NME $M_{\rm exp}({\rm SD2})$ is anomalously small. The smooth trends of the Woods–Saxon energies can be broken by manual adjustments of the single-particle energies close to the proton and/or neutron Fermi surfaces. The resulting basis can be coined "adjusted basis" and it has been used on several occasions in the past calculations to better reproduce the experimentally available single-quasiparticle energies in the neighboring odd-A nuclei. Such adjustments along with adoption of the measured orbital occupancies of the mother and daughter nuclei were done in the case of the $^{76}{\rm Ge} \to {}^{76}{\rm Se}(0^+_{\rm gs})$ double beta transition in [38]. These adjustments resulted in a great improvement of the description of the SD NME and the resulting $\log ft$ of the transition $^{76}{\rm As}(2^-) \to {}^{76}{\rm Se}(0^+_{\rm gs})$ over the previously obtained values (in a slightly adjusted basis) in the works [39,40]. Adjustments have been done also in the works [41–43] with varying success. A more comprehensive study of the effects on the magnitudes of the NMEs coming from the sizes of the single-particle model spaces, adjustments of the single-particle energies and orbital occupancies was discussed in [44].

The GT $\beta^\pm$ sum strengths from the present QRPA calculations satisfy the GT Ikeda sum rule [45]. Then, one can safely say that when the standard Woods–Saxon mean field is used with the BCS occupancies the pnQRPA predicted SD NMEs are consistently much larger than the observed SD NMEs. This difference stems from both the nuclear medium (non-nucleonic and other) effects and the deficiencies of the pnQRPA and the mean field. Disentangling one from the other is not straightforward and easy, but it seems that

in spite of all the fine tuning of the nuclear mean field and the resulting pnQRPA calculation there is always a good portion of the observed NME that cannot be reached by the calculations and this remaining portion could be mostly coming from the nuclear medium effect.

Hence, the presently extracted reduction factors should be considered in the pnQRPA calculations of the SD NMEs related to double beta decays and astro-neutrino interactions The reduction factor, being defined as the ratio of the true NME to the model calculation, depends on how completely the nucleonic and non-nucleonic effects are included explicitly in the model, and thus may be different for other models, like the interacting shell model (ISM) and the interacting boson approximation (IBA2) [30].

Furthermore, it seems that missing couplings of the simple model configurations to more complicated many nucleon configurations and the use of small single-particle model spaces contribute to the reduction factor. The effect on the $M^{0\nu}$ has recently been pointed out in [46].

The reduction factors of $k_{\tau\sigma}$ and $k_{\rm NM}$ are of the same order of magnitude, being in accord with the universal ansatz of the coupling constants of $g_{\rm NN}$ and $g_{\rm N\Delta}$ [47,48]. Then one needs to include explicitly both the $\tau\sigma$ $\rm NN^{-1}$ and $\rm \Delta N^{-1}$ excitations in the calculation to evaluate the relative contributions to the reduction of the SD matrix element. Precise studies of the $\rm SD2^-$ GR strength distribution and the sum of the SD strengths are useful to get the relative contributions of $k_{\tau\sigma}$ and $k_{\rm NM}$.

Similar reduction effects have been discussed in the case of the GT 1^+ NMEs [18] and magnetic moments [48,49] and in shell-model calculations [50]. They were discussed in terms of the isobar effect [47–50].

The reductions found in the SD and GT matrix elements show that the SD transition of the p-wave $\tau\sigma$ mode is much modified in nuclei by the $\tau\sigma$ p-wave polarizations of $\rm NN^{-1}$, $\rm \Delta N^{-1}$ and other correlations, analogously to the case of the GT transitions where the reduction stems from the s-wave $\tau\sigma$ polarizations.

Actually the reduction due to the isobar can be related to the quenching of $g_{\rm A}$ and the summed axial vector strengths. Summed GT strengths observed in $(\rm p,n)/(n,p)$ are claimed to be 0.88 ± 0.06 of the sum rule value, indicating no appreciable quenching effect [51,52] but a shift of the GR strength [53] (see Fig. 1). Recent high-precision $(^3\rm He,t)$ experiment [54] shows a quenching of around 0.5. Summed SD strengths in medium heavy nuclei are not observed, and the SD sum rule is sensitive to the nuclear structure [55]. The summed GT strengths and the GT quenching problem will be discussed elsewhere.

The reduction of the axial vector (AV) 2^- single β matrix elements could have a strong impact on the $0\nu\beta\beta$ experiments [2,4,10]. The AV component of $M^{0\nu}$ depends on $|M(\rm AV)|^2$. Thus, if the renormalization factor of $k_{\rm NM}\approx 0.5$ would also be applied to other multipole AV NMEs, the AV $0\nu\beta\beta$ NME would be reduced with respect to the standard QRPA one by a factor of up to around 4, and the total $0\nu\beta\beta$ NME by a factor around 2, depending on the relative AV component.

It should be noted that the $0\nu\beta\beta$ process is a two-body process with the neutrino potential of H_{ij}, so that the $0\nu\beta\beta$ transition operator is not given by a separable form like the $2\nu\beta\beta$ operator. Since the neutrino potential is of the Coulomb type, $1/r_{ij}$, the NME $M^{0\nu}(2^-)$ via 2^- intermediate states may be approximately given by a product of single $\beta^\pm$ NMEs of $M^-(\rm SD2^-)$ and $M^+(\rm SD2^-)$ via the 2^- intermediate states like the $2\nu\beta\beta$ matrix element $M^{2\nu}$ is given by the GT type NMEs via 1^+ intermediate states. Even one could see something like single-state dominance for the SD 2^- mode as seen for some of the $2\nu\beta\beta$ decaying nuclei for the GT 1^+ mode [56–58]. Actually, low-lying intermediate states contribute to the $2\nu\beta\beta$ NME [4,27,28]. There are 2–5 low lying 2^- states in the present $\beta\beta$ nuclei. Accordingly, the reduction effects on the SD 2^- single $\beta^\pm$ NME may appear also in the $0\nu\beta\beta$ NME as well.

Theoretical model calculations with adequate nucleonic and non-nucleonic correlations are needed to evaluate $M^{0\nu}$ accurately. The present studies of the single $\beta^\pm$ NMEs of $M^\pm(\rm SD2^-)$ and the obtained reduction coefficients may help QRPA and other model calculations of $M^{0\nu}$ and evaluations for the AV weak astro-neutrino–nuclear cross sections and astro-neutrino–nuclear synthesis rates.

Acknowledgements

This work was supported by the Academy of Finland under the Finnish Centre of Excellence Program 2012–2017 (Nuclear and Accelerator Based Program at JYFL). The authors thank Prof. O. Civitarese, Prof. D. Frekers, Prof. M. Harakeh, and Prof. F. Iachello for valuable discussions.

References

[1] H. Ejiri, Phys. Rep. 338 (2000) 265.
[2] J. Vergados, H. Ejiri, F. Šimkovic, Rep. Prog. Phys. 75 (2012) 106301.
[3] S.R. Elliott, P. Vogel, Annu. Rev. Nucl. Part. Sci. 52 (2002) 115.
[4] H. Ejiri, J. Phys. Soc. Jpn. 74 (2005) 2101.
[5] F. Avignone, S. Elliott, J. Engel, Rev. Mod. Phys. 80 (2008) 481.
[6] J. Suhonen, O. Civitarese, Phys. Rep. 300 (1998) 123.
[7] J. Suhonen, O. Civitarese, J. Phys. G, Nucl. Part. Phys. 39 (2012) 124005.
[8] A. Faessler, et al., J. Phys. G, Nucl. Part. Phys. 35 (2008) 075104.
[9] J. Suhonen, O. Civitarese, J. Phys. G, Nucl. Part. Phys. 39 (2012) 085105.
[10] H. Ejiri, in: MEDEX13, APS Conf. Proc. 1572 (2013) 40.
[11] H. Ejiri, J. Engel, N. Kudomi, Phys. Lett. B 530 (2002) 27.
[12] E. Ydrefors, J. Suhonen, Adv. High Energy Phys. 2012 (2012) 373946.
[13] W. Almosly, E. Ydrefors, J. Suhonen, J. Phys. G, Nucl. Part. Phys. 40 (2013) 095201.
[14] H. Ejiri, J.I. Fujita, Phys. Rev. 176 (1968) 1277.
[15] H. Ejiri, Nucl. Phys. A 166 (1971) 594;
H. Ejiri, Nucl. Phys. A 178 (1972) 350;
H. Ejiri, Nucl. Phys. A 211 (1973) 232.
[16] R. Brenn, S.K. Bhattacherjee, C.D. Sprouse, L.E. Young, Phys. Rev. C 10 (1974) 1414.
[17] H. Ejiri, T. Shibata, Phys. Rev. Lett. 35 (1975) 148.
[18] H. Ejiri, J.I. Fujita, Phys. Rep. 38 (1978) 85.
[19] H. Ejiri, Phys. Rev. C 26 (1982) 2628.
[20] J.H. Thies, et al., Phys. Rev. C 86 (2012) 014304.
[21] J.H. Thies, et al., Phys. Rev. C 86 (2012) 045323.
[22] J.H. Thies, et al., Phys. Rev. C 86 (2012) 044309.
[23] P. Puppe, et al., Phys. Rev. C 86 (2012) 044603.
[24] P. Puppe, et al., Phys. Rev. C 84 (2011) 051305(R).
[25] D. Frekers, P. Puppe, J.H. Thies, H. Ejiri, Nucl. Phys. A 916 (2013) 219.
[26] C.J. Guess, et al., Phys. Rev. C 83 (2011) 064318.
[27] H. Ejiri, J. Phys. Soc. Jpn. 78 (2009) 074201.
[28] H. Ejiri, J. Phys. Soc. Jpn. Lett. 81 (2012) 033201.
[29] J. Barea, J. Kotila, F. Iachello, Phys. Rev. C 87 (2013) 014315.
[30] J. Suhonen, O. Civitarese, Phys. Lett. B 725 (2013) 153.
[31] D. Mund, et al., Phys. Rev. Lett. 110 (2013) 172502.
[32] B. Singh, J.L. Rodriguez, S.S.M. Wong, J.K. Tuli, Nucl. Data Sheets 84 (1998) 487.
[33] A. Bohr, B.R. Mottelson, Nuclear Structure, Vol. I, Benjamin, New York, 1969.
[34] J. Suhonen, A. Faessler, T. Taigel, T. Tomoda, Phys. Lett. B 202 (1988) 174.
[35] J. Suhonen, T. Taigel, A. Faessler, Nucl. Phys. A 486 (1988) 91.
[36] J. Suhonen, Nucl. Phys. A 563 (1993) 205.
[37] P. Vogel, M.R. Zirnbauer, Phys. Rev. Lett. 57 (1986) 3148.
[38] J. Suhonen, O. Civitarese, Phys. Lett. B 668 (2008) 277.
[39] M. Kortelainen, J. Suhonen, Phys. Rev. C 75 (2007), 051303(R).
[40] J. Suhonen, M. Kortelainen, Int. J. Mod. Phys. E 17 (2008) 1.
[41] J. Suhonen, Nucl. Phys. A 864 (2011) 63.
[42] J. Suhonen, Phys. Rev. C 87 (2013) 034318.
[43] J. Suhonen, J. Phys. G, Nucl. Part. Phys. 40 (2013) 075102.
[44] J. Suhonen, O. Civitarese, Nucl. Phys. A 847 (2010) 207.
[45] K. Ikeda, S. Fujii, J.I. Fujita, Phys. Lett. 3 (1963) 271.
[46] J.D. Holt, J. Engel, Phys. Rev. C 87 (2013) 064315.
[47] E. Oset, M. Rho, Phys. Rev. Lett. 42 (1979) 47.
[48] A. Bohr, B.R. Mottelson, Phys. Lett. B 100 (1981) 10.
[49] A. Bohr, B.R. Mottelson, Nuclear Structure, Vol. II, New York, 1975.
[50] A. Juodagalvis, D.J. Dean, Phys. Rev. C 72 (2005) 024306.

[51] T. Wakasa, et al., Phys. Rev. C 55 (1997) 2909.
[52] K. Yako, et al., Phys. Lett. B 615 (2005) 193.
[53] G.F. Bertch, I. Hamamoto, Phys. Rev. C 26 (1982) 1323.
[54] D. Frekers, private communication, 2013.
[55] C. Gaarde, et al., Nucl. Phys. A 369 (1981) 258.
[56] M. Bhattacharya, et al., Phys. Rev. C 58 (1998) 1247.
[57] O. Civitarese, J. Suhonen, Phys. Rev. C 58 (1998) 1535.
[58] O. Civitarese, J. Suhonen, Nucl. Phys. A 653 (1999) 321.